

Extrapolation Algorithms for Infrared Divergent Integrals

Elise de Doncker*

Western Michigan University

E-mail: elise.dedoncker@wmich.edu

Junpei Fujimoto

High Energy Accelerator Research Organization (KEK)

E-mail: junpei.fujimoto@kek.jp

Nobuyuki Hamaguchi

Hitachi ICT Business Services, Ltd., Japan

E-mail: nobuyuki.hamaguchi.xr@hitachi.com

Tadashi Ishikawa

High Energy Accelerator Research Organization (KEK)

E-mail: tadashi.ishikawa@kek.jp

Yoshimasa Kurihara

High Energy Accelerator Research Organization (KEK)

E-mail: yoshimasa.kurihara@kek.jp

Marko Ljucovic

Western Michigan University

E-mail: markoljucovic@gmail.com

Yoshimitsu Shimizu

High Energy Accelerator Research Organization (KEK)

E-mail: yohimitsu.shimizu@kek.jp

Fukuko Yuasa

High Energy Accelerator Research Organization (KEK)

E-mail: fukuko.yuasa@kek.jp

This paper describes applications of extrapolation for the computation of coefficients in an expansion of infrared divergent integrals. An extrapolation procedure is performed with respect to a parameter introduced by dimensional regularization. While this treats typical IR singularities at the boundaries of the integration domain, special care needs to be taken in cases where the integrand is singular in the interior of the domain as well as on the boundaries. A double extrapolation is devised for a class of massless vertex integrals. Quadruple precision results are presented, demonstrating high accuracy. The computations are supported by the use of general adaptive integration programs from the QUADPACK package, in iterated integrations with highly singular integrand functions.

3rd Computational Particle Physics Workshop

September 23-25, 2010

Tsukuba, Japan

*Speaker.

1. Introduction

For *infrared* (IR) divergent loop integrals, the integrand functions have non-integrable singularities through vanishing denominators. Based on dimensional regularization, the integral is expanded as a function of a parameter that approaches zero [9].

In this paper we report numerical results for the leading coefficients obtained by convergence acceleration (extrapolation) of a sequence of integral approximations. The methods are explained in detail in [4], where also results are given using double precision arithmetic. In the present paper we give extensive results using quadruple precision and show that in many cases the accuracy can be improved to near the relative machine accuracy.

According to the asymptotic behavior of the integral, we can explore linear or nonlinear extrapolation techniques. The asymptotic expansion gives rise to linear systems of the form

$$S_\ell = \sum_{k=0}^{n-1} a_k \varphi_k(\varepsilon_\ell), \quad 1 \leq \ell \leq n, \quad (1.1)$$

where S_ℓ is generally a scaled version of the integral $I(\varepsilon)$, approximated numerically. A linear system solver or a linear extrapolation method can be used if the φ_k are known functions of ε_ℓ . Otherwise, a nonlinear extrapolation may be suitable, depending on the nature of the φ_k functions.

For (small) $\varepsilon > 0$, the numerical integral approximation may be affected by singular integrand behavior which occurs at the boundaries and/or in the interior of the integration domain. The sample integrals in this paper pertain to classes of one-loop vertex integrals which are two-dimensional, over the unit triangle $\{(x, y) \mid 0 \leq y \leq 1 - x \leq 1\}$. An iterated or repeated numerical integration can be performed efficiently with the general adaptive integration programs DQAGS/DQAG from QUADPACK [14].

The expansions derived symbolically in [9] generally involve hypergeometric functions. We calculate the hypergeometric function numerically in Section 3, using an extrapolation to handle the singularity in the integration interval. In Section 4 we present results for the case of one off-shell ($p_3^2 \neq 0$) and two on-shell ($p_1^2 = p_2^2 = 0$) particles. The coefficients of the divergent terms in the integral expansion are calculated with an extrapolation as the parameter ε introduced by dimensional regularization goes to zero. The integrals in the sequence have integrand singularities on the boundaries of the integration region.

Section 5 addresses IR divergent integrals with one on-shell and two off-shell particles, where integrand singularities may occur in the interior as well as on the boundaries of the integration domain. In this case, the integrals in the extrapolation sequence with respect to ε involves an extrapolation to deal with the interior singularity.

2. Extrapolation

For a sequence $\{S(\varepsilon_\ell)\}$, which converges to the limit $\mathcal{S} = \lim_{\varepsilon_\ell \rightarrow 0} S(\varepsilon_\ell)$, an extrapolation may be performed with the goal of creating sequences which convergence faster than the given sequence, based on its asymptotic expansion

$$S(\varepsilon) \sim \mathcal{S} + A_1 \varphi_1(\varepsilon) + A_2 \varphi_2(\varepsilon) + \dots \quad (2.1)$$

| | | | | | |
|---|---------------------|---------------------|---------------------|---------|--|
| | τ_{00} | | | | |
| 0 | | τ_{01} | | | |
| | τ_{10} | | τ_{02} | | |
| 0 | | τ_{11} | | \dots | $\tau_{\kappa,-1} = 0$ |
| | | \dots | | \dots | $\tau_{\kappa,0} = S_{\kappa}$ |
| | | \dots | | \dots | |
| 0 | | $\tau_{\kappa-1,1}$ | | \dots | $\tau_{\kappa,\lambda+1} = \tau_{\kappa+1,\lambda+1} + \frac{1}{\tau_{\kappa+1,\lambda} - \tau_{\kappa\lambda}}$ |
| | $\tau_{\kappa 0}$ | | $\tau_{\kappa-1,2}$ | | |
| 0 | | $\tau_{\kappa 1}$ | | | |
| | $\tau_{\kappa+1,0}$ | | | | |

Table 1: ε -algorithm table

as $\varepsilon \rightarrow 0$. In the context of series convergence we consider the limit of its partial sums. Some extrapolation methods allow summing divergent series to a value referred to as anti-limit.

A linear extrapolation yields solutions to linear systems of the form

$$S(\varepsilon_{\ell}) = a_0 + a_1 \varphi_1(\varepsilon_{\ell}) + \dots + a_{\nu} \varphi_{\nu}(\varepsilon_{\ell}), \quad \ell = 0, \dots, \nu, \tag{2.2}$$

of order $(\nu + 1) \times (\nu + 1)$ for increasing values of ν [12, 2]. The sequence of ε_{ℓ} may be geometric or another type of sequence that decreases to 0. As an example, Romberg integration relies on the Euler-Maclaurin expansion of the integral as a function of the step size $\varepsilon = h$. Then (2.1) is assumed to be an expansion in even powers of h , for the composite trapezoidal rule values $S(h)$ with $h = 2^{-\ell}$, $\ell \geq 0$. Values for $a_0 \approx \mathcal{S}$ are obtained for successive ν by solving the $(\nu + 1) \times (\nu + 1)$ systems of (2.2) implicitly using the Neville algorithm.

More general sequences of ε include the sequence by Bulirsch, of the form $1/b_{\ell}$ with $b_{\ell} = 2, 3, 4, 6, 8, 12, \dots$ (consisting of powers of 2, alternating with $1.5 \times$ the preceding power of 2). The type of sequence selected influences the stability of the process, which was found more stable with the geometric sequence than with the harmonic sequence (with the Bulirsch sequence in between) [12]. On the other hand there is a trade-off with the computational expense of $S(\varepsilon)$, which may become prohibitive for fast decreasing ε . For the computations in subsequent sections we use scaled versions of b_{ℓ} , e.g., $b_{\ell}/16$.

If the functions of ε in the asymptotic expansion (2.1) are not known, a nonlinear extrapolation or convergence acceleration may be suitable [17, 16, 11, 8]. As an example of a nonlinear extrapolation method, the ε -algorithm [17] implements the sequence-to-sequence transformation by [15] recursively; and can be applied when the φ functions are of the form $\varphi_k(\varepsilon) = \varepsilon^{\beta_k} \log^{\nu_k}(\varepsilon)$, under some conditions on ν_k and β_k and if a geometric sequence is used for ε . The actual form of the underlying ε -dependency does not need to be specified.

Table 1 gives the recurrence of the ε algorithm for a sequence S_{κ} , $\kappa = 0, 1, \dots$ and depicts the layout of the computations in a triangular table.

| PARAMETERS | | | REAL/ IMAG. | EXTRAPOLATED RESULT $\mathcal{S}^{(v)}$ | ESTIM. REL. ERR. $E_k^{(v)}$ | v | TOTAL INT. TIME (s) |
|------------|---|---|----------------|--|---------------------------------|-----|------------------------|
| l | m | n | | | | | |
| 1 | 1 | 1 | REAL | -1.4533220287861469626056457257e-02 | 7.09e-29 | 22 | 7.58e-02 |
| | | | IMAG. | -1.5079644737231007544620688243e-01 | 2.34e-28 | 22 | 9.70e-02 |
| 1 | 2 | 3 | REAL | 8.4177671687810393005426755543e-02 | 2.85e-28 | 22 | 1.26e-01 |
| | | | IMAG. | -2.2902210444669592708392670265e-01 | 1.61e-29 | 22 | 1.20e-01 |
| 2 | 1 | 1 | REAL | 1.08766468837090905178932142e-02 | 7.26e-26 | 21 | 1.08e-01 |
| | | | IMAG. | 2.63893782901542632030862046e-02 | 1.66e-27 | 22 | 1.30e-01 |
| 2 | 3 | 4 | REAL | -2.89056808231506117361219566e-02 | 2.38e-26 | 22 | 1.47e-01 |
| | | | IMAG. | 5.57897846432151278376445447e-02 | 1.44e-27 | 22 | 1.42e-01 |
| 3 | 1 | 2 | REAL | -1.02672179830170273331993276e-02 | 2.94e-27 | 21 | 2.42e-01 |
| | | | IMAG. | -5.65486677646162782923279e-02 | 4.29e-24 | 21 | 2.70e-01 |
| 3 | 4 | 5 | REAL | 8.12135882438810010895282e-03 | 2.58e-24 | 21 | 1.79e-01 |
| | | | IMAG. | -1.27463626362435298394122e-02 | 3.92e-25 | 23 | 2.13e-01 |

Table 2: Integration and extrapolation results for ${}_2F_1(l+1, l+m, l+m+n+1, z+i0)$ for relative integration error tolerance of 10^{-25} and the Bulirsch sequence for extrapolation

3. Hypergeometric function

A representation of the hypergeometric function is given by the Gauss series

$$F(a, b, c; z) = \sum_{k=0}^{\infty} \frac{\Gamma(a+k) \Gamma(b+k)}{\Gamma(c+k)} \frac{z^k}{k!}$$

which has $|z| = 1$ as its circle of convergence and has an analytic continuation defined by the Euler integral [1],

$${}_2F_1(a, b, c; z) = \frac{\Gamma(c)}{\Gamma(b)\Gamma(c-b)} \int_0^1 \frac{t^{b-1}(1-t)^{c-b-1}}{(1-tz)^a} dt, \quad (3.1)$$

$Re c > Re b > 0$, which denotes a one-valued analytic function in the complex plane cut along the real axis from 1 to ∞ .

For a numerical computation where $z \in \mathbb{R}$, we replace z by $z + i\delta$ and evaluate the limit of ${}_2F_1(a, b, c; z + i\delta)$ as $\delta \rightarrow 0$ by solving linear systems of the form (2.2) with $\varphi_k(\delta_\ell) = \delta_\ell^k$, $k = 1, \dots, v$ and $S(\delta_\ell) = {}_2F_1(a, b, c; z + i\delta_\ell)$, $\ell = 0, \dots, v$.

Table 2 lists results for a problem set from [10] where $a = l + 1$, $b = l + m$, $c = l + m + n + 1$ at $z = 10$ (real). The relative error tolerances for the outer and inner integration are set at 10^{-25} and 10^{-26} , respectively. Since b and c are positive integer, the numerator in the integrand is polynomial, so there are no end-point singularities. We use the general adaptive integrator DQAG of QUADPACK for the iterated integrations, with the 7-point Gauss and 15-point Kronrod rules applied on each subinterval in its adaptive partitioning strategy.

Note that the weights and abscissae of the integration rules in DQAG are given to 33 digits and the relative machine accuracy in quadruple precision is of about the same order. Table 2 gives quadruple precision results, extending the (10-digit) accuracy of the double precision calculations reported in [4]. As compiler we use the intel Fortran Composer XE with the -r16 flag. The calculations are run on a Macbook-Pro laptop with 3.06 GHz Intel Core 2 Duo processor and 8 GB memory (Mac OS X Version 10.6.4).

According to (2.2) we obtain $\mathcal{S}^{(v)} \approx a_0$ for the systems of order $(v+1) \times (v+1)$, $v = 1, 2, \dots$. The difference of successive results in $E_a^{(v)} = |\mathcal{S}^{(v)} - \mathcal{S}^{(v-1)}|$ gives a measure of convergence.

Table 2 lists l, m, n followed by the result $\mathcal{S}^{(\nu)}$, the relative measure of convergence $E_r^{(\nu)} = E_a^{(\nu)} / |\mathcal{S}^{(\nu)}|$, the value of ν and the time taken (in seconds) for the integrals $S(\delta_\ell)$, $\ell = 0, \dots, \nu$, needed to obtain the result. The other times in the program are not taken into account, including the system solving time which was measured and found negligible compared to the integration times.

While we could have listed the result obtained after the error falls below 10^{-25} , we instead listed the result with the smallest estimated relative error. As expected, better accuracy is obtained for the smaller values of l, m, n .

4. Asymptotics for one off-shell, two on-shell particles

We first address the IR divergent integral $J_3(p_1^2, p_2^2, p_3^2; n_x, n_y)$ from [9] with one off-shell ($p_3^2 \neq 0$) and two on-shell particles ($p_1^2 = p_2^2 = 0$), which we denote here by $J_3(p_1^2, p_2^2, p_3^2; n_x, n_y; \varepsilon) = \frac{1}{(4\pi)^2} I_3^{n_x, n_y}(\varepsilon)$, with

$$\begin{aligned} I_3^{n_x, n_y}(\varepsilon) &= \frac{\varepsilon \Gamma(-\varepsilon)}{(4\pi\mu_R^2)^\varepsilon} \int_0^1 dx \int_0^{1-x} dy \frac{x^{n_x} y^{n_y}}{(-p_3^2 xy - i0)^{1-\varepsilon}} \\ &= \varepsilon \Gamma(-\varepsilon) \left(\frac{-\tilde{p}_3^2}{4\pi\mu_R^2} \right)^\varepsilon \frac{1}{-p_3^2} \frac{B(n_x + \varepsilon, n_y + \varepsilon)}{n_x + n_y + 2\varepsilon}. \end{aligned} \quad (4.1)$$

where $\tilde{p}_3^2 = p_3^2 + i0$ and μ_R^2 is a renormalization constant (which we will replace by $\mu_R^2 \leftarrow e^{\gamma_E} / (4\pi)$, γ_E is Euler's constant). The introduction of the parameter ε pertains to the dimension regularization technique [13].

When $n_x = \eta \neq 0$ or $n_y \neq 0$, we have

$$\begin{aligned} I_3^{\eta, 0}(\varepsilon) &\sim \frac{1}{p_3^2} \left(\frac{C_{-1}}{\varepsilon} + C_0 + \mathcal{O}(\varepsilon) \right) \quad \text{with} \\ C_{-1} &= \frac{1}{\eta}, \quad C_0 = -\frac{2}{\eta^2} + \frac{1}{\eta} \left(\ln(-p_3^2) - \sum_{j=1}^{\eta-1} \frac{1}{j} \right). \end{aligned} \quad (4.2)$$

A linear extrapolation can be formulated using systems of the form (2.2) with $S_\ell(\varepsilon_\ell) = \varepsilon_\ell \hat{I}(\varepsilon_\ell)$ where $\hat{I}(\varepsilon_\ell) \approx I_3^{\eta, 0}(\varepsilon)$ and $\varphi_k(\varepsilon_\ell) = \varepsilon_\ell^k$.

Table 3 displays results for the real parts of the coefficients C_{-1} and C_0 in the expansion, for $n_x = \eta = 2$ and $n_y = 0$. In view of the integrand singularity along $y = 0$ through the factor $y^{\varepsilon-1}$ where the exponent approaches -1, and a second derivative singularity along $x = 0$ through the factor $x^{1+\varepsilon}$ in (4.1), we perform the calculation of $\hat{I}(\varepsilon_\ell)$ with the program DQAGS of QUADPACK [14], which is equipped to deal with these end-point singularities. DQAGS uses the 7-point Gauss and 15-point Kronrod rule on each subinterval created in its adaptive subdivision strategy.

We set the requested relative accuracies to 5×10^{-24} for the outer and 10^{-25} for the inner integral. Table 3 lists the sequence of extrapolation results and shows how much accuracy can be reached. (After that, the accuracy no longer improves; i.e., stagnates for a few steps and decreases). The difference between successive results provides a good estimate of the convergence. For this problem it usually gives a somewhat conservative bound for the actual error, in the sense that the difference with the result of the previous step is in fact a measure of the error in the previous step.

| ν | INTEGRATION | | EXTRAPOLATION RESULTS | |
|--------------|-------------|----------|-----------------------------------|---------------------------------|
| | # EVALS | TIME (s) | C_{-1} | C_0 |
| 1 | 1125075 | 1.10 | 0.8707294126792779500928011356924 | -0.5511174754172542062710316596 |
| 2 | 1349535 | 1.34 | 0.3457684478555631741492957488633 | 3.1236092783487492253335060482 |
| 3 | 1348875 | 1.33 | 0.5262024637357823738306365020734 | 0.7779670719058996294760762565 |
| 4 | 134 9355 | 1.33 | 0.4976817315764365660976698223580 | 1.3769024472521615918683765304 |
| 5 | 1324125 | 1.30 | 0.5001453140694736901417736134445 | 1.3030216329875385877494858112 |
| 6 | 1274625 | 1.26 | 0.5000001921131322347567104032762 | 1.3025651116288535549087530061 |
| 7 | 127 4625 | 1.25 | 0.4999999959467322713652940448364 | 1.302585091321435704903401609 |
| 8 | 1225125 | 1.21 | 0.49999999993260163866288358759 | 1.3025850932043285642085160900 |
| 9 | 1200375 | 1.18 | 0.500000000000053069685193174512 | 1.3025850929940632251166716065 |
| 10 | 1175625 | 1.16 | 0.49999999999999722450728860463 | 1.3025850929940632251166716065 |
| 11 | 1101375 | 1.08 | 0.50000000000000001089023336541 | 1.3025850929940455873126312708 |
| 12 | 1076625 | 1.06 | 0.49999999999999997158886319 | 1.3025850929940456843793808956 |
| 13 | 1037475 | 1.02 | 0.50000000000000000000000564493 | 1.3025850929940456840169987640 |
| 14 | 1037475 | 1.00 | 0.49999999999999999999999992988 | 1.3025850929940456840179932776 |
| 15 | 952425 | 0.90 | 0.4999999999999999999999999980 | 1.3025850929940456840179914927 |
| Total time : | | 20.31 | Exact : | 0.5 |

Table 3: Integration performance (DQAGS)², for rel. integration error tolerances 5×10^{-24} (outer), 10^{-25} (inner); $n_x = \eta = 2$, $n_y = 0$ and $p_3^2 = 100$. Extrapolated real values.

The final accuracy reached for C_{-1} is about 2×10^{-30} (absolute error), 4×10^{-30} (relative error). The accuracy in C_0 lags behind and reaches about 4×10^{-26} (absolute) or 3×10^{-26} (relative error).

When $n_x = n_y = 0$ we have

$$I_3^{0,0}(\varepsilon) \sim \frac{1}{p_3^2} \left(\frac{C_{-2}}{\varepsilon^2} + \frac{C_{-1}}{\varepsilon} + C_0 + \mathcal{O}(\varepsilon) \right) \quad \text{with}$$

$$C_{-2} = 1, \quad C_{-1} = \ln(-p_3^2), \quad C_0 = -\frac{\pi^2}{12} + \frac{1}{2} \ln^2(-p_3^2). \quad (4.3)$$

With relative tolerances of 10^{-26} for the outer and 5×10^{-27} for the inner integrations, we obtain the best relative accuracies for C_{-2} , C_{-1} and C_0 at $\nu = 15$, of 7.88e-25, 4.33e-22 and 4.0e-19, respectively. Note that the best accuracies for this problem obtained in double precision with integration tolerances of 10^{-13} (outer), 5×10^{-14} (inner) are reported in [4] as 3.06e-12, 1.44e-10 and 7.99e-09 at $\nu = 11$. The latter can also be compared with our 10^{-26} , 5×10^{-27} quadruple precision result at $\nu = 11$, which yields 3.18e-14, 3.04e-12 and 5.24e-10, respectively.

5. Asymptotics for one on-shell, two off-shell particles

In the case of one on-shell ($p_1^2 = 0$) and two off-shell ($p_2^2 \neq 0$, $p_3^2 \neq 0$) particles, the IR divergent integral is

$$J_3(0, p_2^2, p_3^2; n_x, n_y; \varepsilon) = \frac{1}{(4\pi)^2} J_3(0, 0, p_3^2; n_x, n_y; \varepsilon) {}_2F_1(1, 1 - \varepsilon, 2 + n_x; \frac{p_3^2 - p_2^2}{\tilde{p}_3^2}) \frac{n_x + \varepsilon}{n_x + 1} \quad (5.1)$$

$$= \frac{1}{(4\pi)^2} \frac{\varepsilon \Gamma(-\varepsilon)}{(4\pi \mu_R^2)^\varepsilon} \int_0^1 dx \int_0^{1-x} dy \frac{x^{n_x} y^{n_y}}{(-(p_3^2 - p_2^2)xy - p_2^2 y(1-y) - i0)^{1-\varepsilon}}. \quad (5.2)$$

For $n_x = n_y = 0$ we use the expansion

$$J_3(0, p_2^2, p_3^2; n_x, n_y; \varepsilon) \sim \frac{\tilde{C}_{-1}}{\varepsilon} + \tilde{C}_0 + \mathcal{O}(\varepsilon) \quad (5.3)$$

with

$$\begin{aligned} \tilde{C}_{-1} &= -\frac{1}{(4\pi)^2 p_3^2} \frac{\ln(1-z)}{z} \\ \tilde{C}_0 &= -\frac{1}{(4\pi)^2 p_3^2} \left(C_{-1} \frac{\ln(1-z)}{z} + \frac{\ln^2(1-z)}{2z} \right) \end{aligned}$$

with $z = \frac{p_3^2 - p_2^2}{\tilde{p}_3^2}$ and the C_{-1} coefficient of (4.3). In the subsections below we will give results for two methods for the computation of $J_3(0, p_2^2, p_3^2; n_x, n_y; \varepsilon)$, the first based on (5.1) and the second on (5.2).

5.1 Computation of $J_3(0, p_2^2, p_3^2; n_x, n_y)$ with hypergeometric function

We intend to perform an extrapolation with respect to the parameter ε for dimensional regularization. According to (5.1), each term in the extrapolation sequence consists of a double integral multiplied with a hypergeometric function, both dependent on ε . We calculate the hypergeometric function numerically using the δ extrapolation of Section 3, to alleviate the characteristic non-integrable singularity on the real axis when it occurs inside the integration interval.

Here $z = \frac{p_3^2 - p_2^2}{\tilde{p}_3^2}$ in the fourth argument of ${}_2F_1$ in (5.1) is replaced by $z + i\delta$. Thus in this process we need to evaluate sequences of hypergeometric functions of the form

$${}_2F_1(1, 1 - \varepsilon_\ell, 2 + n_x; \frac{p_3^2 - p_2^2}{\tilde{p}_3^2} + i\delta_\kappa), \quad \kappa = 1, 2, \dots$$

for $\varepsilon = 1, 2, \dots$. The number of κ -values needed depends on the convergence for each (fixed) ε . As the exponents $b - 1 = -\varepsilon_\ell$ and $c - b - 1 = n_x + \varepsilon_\ell$ in the integrand numerator $t^{b-1}(1-t)^{c-b-1}$ of the Euler integral (3.1) are non-integer, we use the QUADPACK program DQAGS to treat the integrand behavior at the end-points.

Extrapolated (real part) results for \tilde{C}_{-1} and \tilde{C}_0 in (5.3) and actual absolute errors are listed in Table 4. By setting $p_2^2 = 40$, $p_3^2 = -100$, for the purpose of a numerical example, we have that $Re(z) = 1.4$, so that the hypergeometric function has an integrand singularity at $t = 1/1.4$ in the interior of the integration interval $(0, 1)$.

The relative error tolerances for DQAGS were 10^{-26} for the outer integration and 5×10^{-27} for the inner integrals. The maximum number of subdivisions was set to 150 for J_3 in both directions and to 300 for ${}_2F_1$. For the dimensional regularization extrapolation, the Bulirsch sequence was used starting at 3, i.e., 3, 4, 6, \dots

For $p_3^2 = -100$, the integral in (4.1) is real and is multiplied with the (complex) value of the hypergeometric function. The real and imaginary parts of the latter are currently computed separately which, for the real part, took between about 0.44 and 0.55 seconds, and for the imaginary part between 0.33 and 0.41 seconds. Thus the time for the hypergeometric function computation for each equation in the linear system is under a second and is dominated by the times for the

| v | TIME INT.(S) | EXTRAPOLATION RESULTS | | | |
|------|-----------------|----------------------------------|----------|-------------------------------|----------|
| | | \tilde{C}_{-1} | ERROR | \tilde{C}_0 | ERROR |
| 4 | 3.47 | -4.2192812666950192419664334e-05 | 7.47e-07 | -3.7121279333017303070237e-04 | 2.39e-05 |
| 5 | 3.47 | -4.1395889404540049511801909e-05 | 5.04e-08 | -3.9751126098970774666184e-04 | 2.42e-06 |
| 6 | 3.41 | -4.1448485840565542759037853e-05 | 2.21e-09 | -3.9493403562445857754728e-04 | 1.59e-07 |
| 7 | 3.39 | -4.1446205836959577424975383e-05 | 7.16e-11 | -3.9510047588769404693383e-04 | 7.45e-09 |
| 8 | 3.33 | -4.1446278988182334267440660e-05 | 1.53e-12 | -3.9509279500930457847498e-04 | 2.32e-10 |
| 9 | 3.30 | -4.1446277437326639980970560e-05 | 2.43e-14 | -3.9509303229022580430491e-04 | 5.25e-12 |
| 10 | 3.53 | -4.1446277461859729880198253e-05 | 2.56e-16 | -3.9509302696654529617250e-04 | 7.97e-14 |
| 11 | 3.86 | -4.1446277461602157717453434e-05 | 2.01e-18 | -3.9509302704716538311163e-04 | 8.86e-16 |
| 12 | 3.75 | -4.1446277461604182432081146e-05 | 1.05e-20 | -3.9509302704627248396080e-04 | 6.66e-18 |
| 13 | 3.81 | -4.1446277461604171849957952e-05 | 4.14e-23 | -3.9509302704627918244479e-04 | 3.67e-20 |
| 14 | 3.77 | -4.1446277461604171891430927e-05 | 1.08e-25 | -3.9509302704627914557531e-04 | 1.37e-22 |
| 15 | 3.81 | -4.1446277461604171891322514e-05 | 3.19e-28 | -3.9509302704627914571332e-04 | 5.44e-25 |
| 16 | 3.76 | -4.1446277461604171891322881e-05 | 4.87e-29 | -3.9509302704627914571267e-04 | 1.12e-25 |
| 17 | 3.82 | -4.1446277461604171891322692e-05 | 1.39e-28 | -3.9509302704627914571315e-04 | 3.69e-25 |
| 18 | 3.78 | -4.1446277461604171891323096e-05 | 2.63e-28 | -3.9509302704627914571171e-04 | 1.07e-24 |
| 19 | 3.82 | -4.1446277461604171891322859e-05 | 2.63e-29 | -3.9509302704627914571292e-04 | 1.40e-25 |
| Ex : | | -4.1446277461604171891322832e-05 | | -3.9509302704627914571278e-04 | |

Table 4: Integration performance (DQAGS)², for rel. integration error tolerances 10^{-26} (outer), 5×10^{-27} (inner); vertex with one on-shell, two off-shell particles, $n_x = n_y = 0$ and $p_2^2 = 40$, $p_3^2 = -100$. Extrapolated real values and corresponding actual absolute errors.

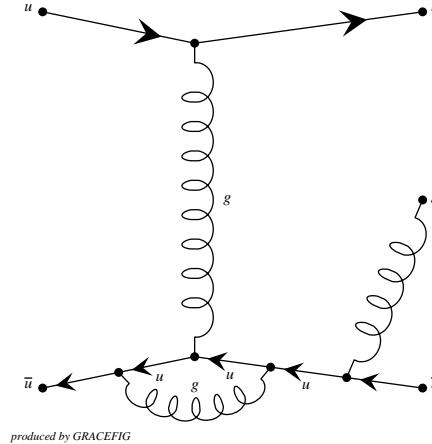


Figure 1: $qq \rightarrow qqg$ diagram. The vertical gluon propagator carries p_3^2 and the u-quark emitting a gluon carries p_2^2 .

integrations of J_3 in (4.1) (given in Table 4). The total time spent in the double integration is 68.3 seconds (including that of the first three steps, which are not shown).

A sample diagram for the vertex correction with one on-shell and two off-shell particles is depicted in Figure 1 for the in $qq \rightarrow qqg$ interaction. Here the vertical gluon propagator carries p_3^2 and the u-quark emitting a gluon carries p_2^2 . Note that the vertical gluon propagator can be virtual so that the square of its momentum becomes negative.

5.2 Computation of $J_3(0, p_2^2, p_3^2; n_x, n_y)$ using direct integration

In this section we calculate the integral in (5.2) directly, which becomes highly singular at $y = 0$ as $\varepsilon \rightarrow 0$ and non-integrable for $\varepsilon = 0$, in view of the factor $y^{\varepsilon-1}$ in the integrand $\frac{y^{\varepsilon-1}}{(-D)^{1-\varepsilon}}$. It

can be seen that $(p_3^2 - p_2^2)x + p_2^2(1 - y) = 0$ along a line that goes through $(p_2^2 / (p_2^2 - p_3^2), 0)$ and $(0, 1)$. Thus for $p_2^2 = 40$, $p_3^2 = -100$, this line runs through the integration domain, where it causes a singularity that becomes non-integrable as $\varepsilon \rightarrow 0$.

According with previous work (e.g., [6, 7, 5, 18, 3]), we will replace $i0$ by $i\delta$ in the integrand denominator of (5.2). This leads to integrals of the form

$$I_3(\varepsilon, \delta) = \frac{1}{(4\pi)^2} \frac{\varepsilon \Gamma(-\varepsilon)}{(4\pi\mu_R^2)^\varepsilon} \int_0^1 dx \int_0^{1-x} dy \frac{x^{n_x} y^{n_y}}{(-(p_3^2 - p_2^2)xy - p_2^2y(1 - y) - i\delta)^{1-\varepsilon}}$$

$$\sim \frac{\tilde{C}_{-1}(\delta)}{\varepsilon} + \tilde{C}_0(\delta) + \mathcal{O}(\varepsilon) \quad (5.4)$$

to be computed in an extrapolation as $\delta \rightarrow 0$, for each (fixed) value of the dimensional regularization parameter ε . The expansion (5.3) or (5.4) with respect to ε justifies a linear extrapolation. However, a linear extrapolation as $\delta \rightarrow 0$ is not suited, as it cannot be assumed that the underlying expansion is in integer powers of δ .

Preliminary results are shown in Tables 5-6 for the real and the imaginary parts, respectively. We employ a sequence of $\delta_\kappa = 2^{-8-\kappa}$, $\kappa = 0, 1, \dots$ in an extrapolation using the ε -algorithm of Wynn [15, 17]. The current implementation incorporates a simple strategy with an extrapolation sequence of fixed length (= 18), which should be improved with a termination criterion based on the estimated errors. Geometric sequences of δ with a smaller ratio should also be tested. For the extrapolation with respect to ε the Bulirsch sequence 3, 4, 6, ... is used.

| ν | C_{-1} | ERROR | C_0 | ERROR |
|-------|----------------------|----------|---------------------|----------|
| 4 | -4.2192812666986e-05 | 7.47e-07 | -3.712127933292e-04 | 2.39e-05 |
| 5 | -4.1395889404493e-05 | 5.04e-08 | -3.975112609915e-04 | 2.42e-06 |
| 6 | -4.1448485840595e-05 | 2.21e-09 | -3.949340356225e-04 | 1.59e-07 |
| 7 | -4.1446205836943e-05 | 7.16e-11 | -3.951004758891e-04 | 7.45e-09 |
| 8 | -4.1446278988175e-05 | 1.53e-12 | -3.950927950097e-04 | 2.23e-10 |
| 9 | -4.1446277437321e-05 | 2.43e-14 | -3.950930322905e-04 | 5.24e-12 |
| 10 | -4.1446277461827e-05 | 2.23e-16 | -3.950930269725e-04 | 7.38e-14 |
| 11 | -4.1446277461600e-05 | 3.96e-18 | -3.950930270436e-04 | 2.69e-16 |
| Ex: | -4.1446277461604e-05 | | -3.950930270463e-04 | |

Table 5: Integration performance (DQAGS)², for rel. integration error tolerances 10^{-15} (outer), 10^{-16} (inner); Vertex with one on-shell, two off-shell particles, $n_x = n_y = 0$ and $p_2^2 = 40$, $p_3^2 = -100$. Extrapolated real parts and actual absolute errors.

| ν | C_{-1} | ERROR | C_0 | ERROR |
|-------|--------------------|----------|-------------------|----------|
| 1 | 0.758010428109e-04 | 6.63e-05 | 9.62356140022e-04 | 4.38e-04 |
| 2 | 1.464854199104e-04 | 4.38e-06 | 4.67565500325e-04 | 5.66e-05 |
| 3 | 1.420636477897e-04 | 3.90e-08 | 5.25048537895e-04 | 4.91e-07 |
| 4 | 1.421000460091e-04 | 2.58e-09 | 5.24284175287e-04 | 8.47e-08 |
| 5 | 1.421026578481e-04 | 3.01e-11 | 5.24197984601e-04 | 1.48e-09 |
| 6 | 1.421026279735e-04 | 2.13e-13 | 5.24199448458e-04 | 1.55e-11 |
| 7 | 1.421026277585e-04 | 2.16e-15 | 5.24199464154e-04 | 2.32e-13 |
| 8 | 1.421026277612e-04 | 5.84e-16 | 5.24199463865e-04 | 5.64e-14 |
| Ex: | 1.421026277606e-05 | | 5.24199463922e-04 | |

Table 6: Integration performance (DQAGS)², for rel. integration error tolerances 10^{-15} (outer), 10^{-16} (inner); Vertex with one on-shell, two off-shell particles, $n_x = n_y = 0$ and $p_2^2 = 40$, $p_3^2 = -100$. Extrapolated imaginary parts and actual absolute errors.

The requested accuracies for DQAGS are 10^{-15} for the outer and 10^{-16} for the inner integrations. The real and imaginary parts are calculated separately as the QUADPACK programs currently do not handle complex functions. The imaginary parts converge more quickly than the real parts for this problem. We list the steps 1 to 8; the last for a 9×9 system. The results do not improve after that. Note that it is not necessary to solve the previous systems, but the integrals need to be calculated to set up the system. Successive systems can be solved to provide an estimate of the error.

Conclusions

We use 1D integration programs from QUADPACK for the iterated integrations underlying the extrapolation processes for IR divergent vertex integrals. We give preliminary results in quadruple precision which demonstrate that the calculations result in high accuracy. For the vertex computation with one on-shell and two off-shell particles we devise a double extrapolation, since problems are introduced with integrand singularities in the interior of the domain as well as on the boundaries. Many integrals result, which makes the computation a good candidate for parallelization, especially when applied to more complicated diagrams and possibly in higher precision.

More work is needed for improvements and extensions of these strategies and analysis of the numerical methods and results. This computation is a step toward a more automatic numerical handling of various types of loop integrals, thereby circumventing the need for a precise knowledge of the location and structure of the singularities.

References

- [1] ABRAMOWITZ, M., AND STEGUN, I. S. *Handbook of Mathematical Functions*. Dover Publications, Inc., New York, 1965.
- [2] BREZINSKI, C. A general extrapolation algorithm. *Numerische Mathematik* 35 (1980), 175–187.
- [3] DE DONCKER, E., FUJIMOTO, J., HAMAGUCHI, N., ISHIKAWA, T., KURIHARA, Y., SHIMIZU, Y., AND YUASA, F. Transformation, reduction and extrapolation techniques for Feynman loop integrals. *Springer Lecture Notes in Computer Science (LNCS) 6017* (2010), 139–154.
- [4] DE DONCKER, E., FUJIMOTO, J., HAMAGUCHI, N., ISHIKAWA, T., KURIHARA, Y., SHIMIZU, Y., AND YUASA, F. Quadpack computation of Feynman loop integrals. *Journal of Computational Science (JoCS)* (2011), doi:10.1016/j.jocs.2011.06.003.
- [5] DE DONCKER, E., LI, S., SHIMIZU, Y., FUJIMOTO, J., AND YUASA, F. Numerical computation of a non-planar two-loop vertex diagram. In *LoopFest V, Stanford Linear Accelerator Center* (2006). <http://www-conf.slac.stanford.edu/loopfestv/proc/present/DEDONCKER.pdf>.
- [6] DE DONCKER, E., SHIMIZU, Y., FUJIMOTO, J., AND YUASA, F. Computation of loop integrals using extrapolation. *Computer Physics Communications* 159 (2004), 145–156.
- [7] DE DONCKER, E., SHIMIZU, Y., FUJIMOTO, J., YUASA, F., CUCOS, L., AND VAN VOORST, J. Loop integration results using numerical extrapolation for a non-scalar integral. *Nuclear Instruments and Methods in Physics Research Section A* 539 (2004), 269–273. hep-ph/0405098.
- [8] FORD, W., AND SIDI, A. An algorithm for the generalization of the Richardson extrapolation process. *SIAM J. Numer. Anal.* 24 (1987), 1212–1232.

- [9] KURIHARA, Y. Dimensionally regularized one-loop tensor integrals with massless internal particles. *Eur. Phys. J. C* 45 (2005), 427. hep-ph/0504251 v3.
- [10] KURIHARA, Y., AND KANEKO, T. Numerical contour integration for loop integrals. *Computer Physics Communications* 174, 7 (2006), 530–539. hep-ph/0503003 v1.
- [11] LEVIN, D., AND SIDI, A. Two classes of non-linear transformations for accelerating the convergence of infinite integrals and series. *Appl. Math. Comp.* 9 (1981), 175–215.
- [12] LYNESS, J. N. Applications of extrapolation techniques to multidimensional quadrature of some integrand functions with a singularity. *Journal of Computational Physics* 20 (1976), 346–364.
- [13] MUTA, T. *Foundations of Quantum Chromodynamics: An Introduction to Perturbative Methods in Gauge Theories*. World Scientific, 2008. Lecture Notes in Physics, Vol. 70.
- [14] PIESSENS, R., DE DONCKER, E., ÜBERHUBER, C. W., AND KAHANER, D. K. *QUADPACK, A Subroutine Package for Automatic Integration*. Springer Series in Computational Mathematics. Springer-Verlag, 1983.
- [15] SHANKS, D. Non-linear transformations of divergent and slowly convergent sequences. *J. Math. and Phys.* 34 (1955), 1–42.
- [16] SIDI, A. Convergence properties of some nonlinear sequence transformations. *Math. Comp.* 33 (1979), 315–326.
- [17] WYNN, P. On a device for computing the $e_m(s_n)$ transformation. *Mathematical Tables and Aids to Computing* 10 (1956), 91–96.
- [18] YUASA, F., ISHIKAWA, T., FUJIMOTO, J., HAMAGUCHI, N., DE DONCKER, E., AND SHIMIZU, Y. Numerical evaluation of Feynman integrals by a direct computation method. In *XII Adv. Comp. and Anal. Tech. in Phys. Res.* (2008). PoS (ACAT08) 122; arXiv:0904.2823.